

# Tree tensor network states represent low-energy states faithfully

Thomas Barthel

*National Quantum Laboratory, University of Maryland, College Park, MD 20742, USA*

*Department of Physics, University of Maryland, College Park, MD 20742, USA and*

*Department of Physics and DQC, Duke University, Durham, NC 27708, USA*

(Dated: November 27, 2025)

Extending corresponding results for matrix product states [Verstraete and Cirac, PRB **73**, 094423 (2006); Schuch et al. PRL **100**, 030504 (2008)], it is shown how the approximation error of tree tensor network states (TTNS) can be bounded using Schmidt spectra or Rényi entanglement entropies of the target quantum state. Conversely, one obtains bounds on TTNS bond dimensions needed to achieve a specific approximation accuracy. For tree lattices, the result implies that efficient TTNS approximations exist if  $\alpha < 1$  Rényi entanglement entropies for single-branch cuts obey an area law, as in ground and low-energy states of certain gapped systems.

## 1. Introduction and main result

*Tensor network states* (TNS) [1–12] are an important tool for the investigation of strongly correlated quantum many-body systems. Numerical TNS algorithms allow for the study of ground states, finite-temperature states, response functions, non-equilibrium dynamics, driven-dissipative systems, and quantum circuits. The basic idea is to approximate many-body states by a network of partially contracted tensors. The tensors are assigned to vertices of a graph and carry physical indices. In addition, neighboring tensors share common bond indices that we sum over to obtain the quantum state. When the network structure of the TNS aligns well with the entanglement structure of the target state, small bond dimensions (small numbers of effective degrees of freedom) suffice for accurate TNS approximations, thus bypassing the curse of dimensionality.

Following Steve White’s development of the *density matrix renormalization group* (DMRG) for one-dimensional systems [5, 13], it was realized [14, 15] that DMRG is actually a variational algorithm for *matrix product states* (MPS) [2, 4, 15, 16]. Around the same time, the DMRG idea was adapted for the simulation of quantum systems on tree graphs [17–19], and it turns out that this yields a variational algorithm for *tree tensor network states* (TTNS), which have precursors in real-space renormalization group schemes [20–23] and had previously been considered in analytical work [24]. Use and method development accelerated after TTNS algorithms were formulated in the language of tensor networks [25–28]. Both being loop-free classes of tensor networks, the MPS and TTNS varieties are closed sets [29] and the variational optimization is free of barren plateaus [30, 31].

As previously mentioned, the TNS tensors carry physical indices like  $\sigma_i = \uparrow, \downarrow$  that label basis states of local quantum degrees of freedom like a spin-1/2. In addition, the tensors carry the auxiliary *bond indices*  $\mu_i = 1, \dots, M_i$ . The computational efficiency critically depends on the required bond dimensions  $M_i$  needed to achieve a specific approximation accuracy. For MPS, Refs. [32, 33] established upper and lower bounds on bond dimensions, using Schmidt spectra or Rényi entanglement entropies of the target quantum state. Given that TTNS have found many applications for the simulation of strongly correlated systems spanning condensed matter [26, 27, 34–47], nuclear and particle physics [48, 49], quantum chemistry [27, 28, 50–52], and quantum computation [53–56], it is important to devise corresponding bounds for TTNS.

This work establishes lower and upper bounds on TTNS approximation errors and required TTNS bond dimensions based on Schmidt spectra and Rényi entanglement entropies [57, 58] of the target state.

**Main result.**— Consider a tree graph with  $N$  vertices, an assignment of quantum degrees of freedom to vertices of the graph, and a target state  $|\psi\rangle$  of the composite system. Let  $\lambda_{i,1} \geq \lambda_{i,2} \geq \dots \geq 0$  denote the Schmidt coefficients of  $|\psi\rangle$  for the bipartition of the system that corresponds to cutting edge  $i$ , with  $S_{\alpha,i} = \frac{1}{1-\alpha} \ln \sum_{\mu} \lambda_{i,\mu}^{2\alpha}$  being the associated  $\alpha$ -Rényi entanglement entropy.

(a) There exists a TTNS approximation  $|\psi_{\text{TTNS}}\rangle$  with bond dimensions  $M_1, \dots, M_{N-1}$  that achieves an approximation accuracy  $\delta := \|\psi - \psi_{\text{TTNS}}\|^2$  bounded by

$$1 - \min_i \left( \frac{M_i}{S_{\tilde{\alpha},i}} \right)^{1-\frac{1}{\tilde{\alpha}}} \leq \max_i \varepsilon_i(M_i) \leq \delta \leq \sum_i \varepsilon_i(M_i) \leq \sum_i \left( \frac{e^{S_{\alpha,i}}}{M_i - 1} \right)^{\frac{1}{\alpha}-1}, \quad (1)$$

$$\text{where } \varepsilon_i(M_i) := \sum_{\mu > M_i} \lambda_{i,\mu}^2 \quad (2)$$

is the bond- $i$  truncation error, and the Rényi parameters can be freely chosen in the ranges  $\tilde{\alpha} > 1$  and  $1 > \alpha \geq \varepsilon_i M_i / (M_i - 1 - \varepsilon_i) \approx \varepsilon_i$ , respectively.

(b) There exists a TTNS approximation  $|\psi_{\text{TTNS}}\rangle$  with approximation accuracy  $\delta := \|\psi - \psi_{\text{TTNS}}\|^2 \leq (N-1)\epsilon$  and bond dimensions  $M_1, \dots, M_{N-1}$  bounded by

$$e^{S_{\tilde{\alpha},i}} (1 - \delta)^{\frac{\tilde{\alpha}}{\tilde{\alpha}-1}} \leq \min\{M \mid \varepsilon_i(M) \leq \delta\} \leq M_i \leq \min\{M \mid \varepsilon_i(M) \leq \epsilon\} \leq e^{S_{\alpha,i}} \left( \frac{1}{\epsilon} \right)^{\frac{\alpha}{1-\alpha}} + 1 \quad (3)$$

for any  $\tilde{\alpha} > 1$  and  $\alpha$  with  $1 > \alpha \geq \epsilon M_i / (M_i - 1 - \epsilon) \approx \epsilon$ .

Section 2 introduces notations and conventions. Section 3 describes how to construct exact TTNS representations for any target state  $|\psi\rangle$  by a sequence of singular value decompositions (SVD). Section 4 explains the lower bounds in Eqs. (1) and (3) in terms of truncation errors. Section 5 briefly discusses a simple and instructive TTNS approximation scheme that leads to an upper bound on the approximation accuracy similar to Eq. (1), with the caveat that the bound depends on Schmidt spectra of truncated states instead of those of the target state  $|\psi\rangle$ . Starting from the exact TTNS representation, Section 6 proves the upper bounds in the main result in terms of truncation errors. Finally, Section 7 explains the bounds in terms of Rényi entanglement entropies. Section 8 provides a conclusion and comments on entanglement area laws for quantum systems on tree graphs.

## 2. Notations and conventions

Consider a quantum many-body system with  $N$  sites. Each site  $i$  is associated with a Hilbert space of dimension  $d_i$  and orthonormal single-site basis states

$$|\sigma_i\rangle \quad \text{with} \quad \sigma_i = 1, \dots, d_i. \quad (4)$$

For distinguishable  $d_i$ -level systems, the total Hilbert space  $\mathcal{H}$  is the tensor product space  $\bigotimes_{i=1}^N \mathbb{C}^{d_i}$ . For identical fermions, we are restricted to the anti-symmetric subspace with Fock-state basis  $\{|\sigma_1, \dots, \sigma_N\rangle\}$  [59–63]. For bosons, we may limit maximum occupation numbers in accordance with energy constraints.

For corresponding TTNS, the physical sites are assigned to the vertices of a tree graph with vertex  $i = N$  chosen as the root and all other vertex indices decreasing with increasing graph distance from the root. An example is shown in Fig. 1a. Edges of the graph are directed from parents to children, where edge  $i$  is pointing towards vertex  $i$ . Cutting edge  $i$  decomposes the tree graph into the branch  $\mathcal{L}(i)$ , containing vertex  $i$  and its descendants, and the remainder  $\mathcal{R}(i) = [1, N] \setminus \mathcal{L}(i)$ .

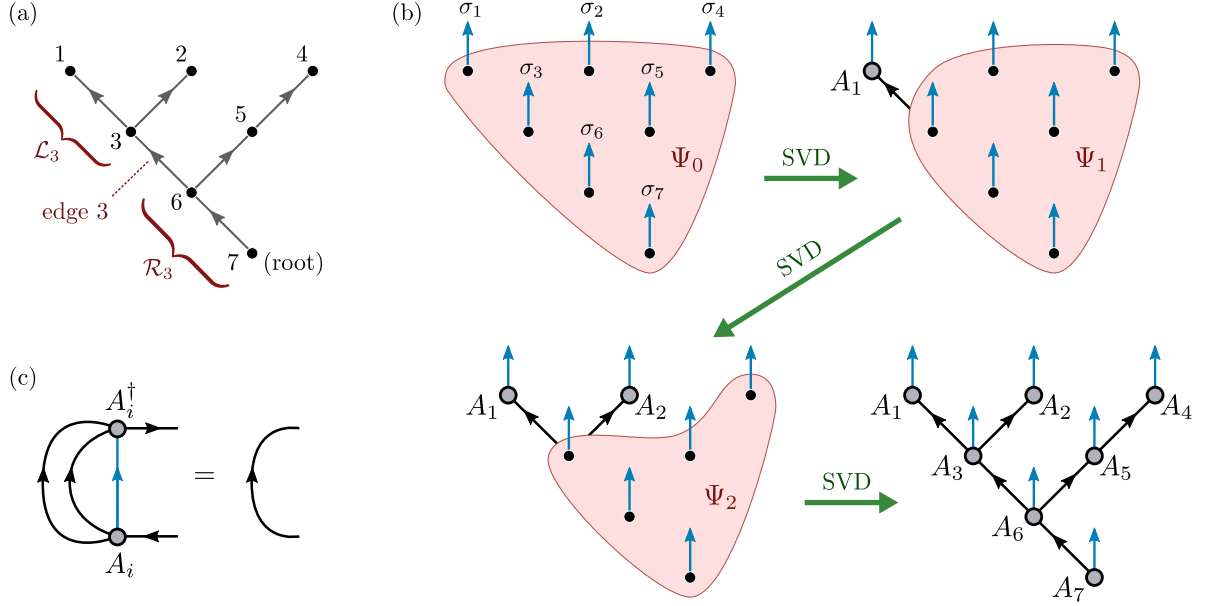


FIG. 1. For an exact TTNS representation of a target state (8) with expansion coefficients  $\Psi^{\sigma_1, \dots, \sigma_N}$ , (a) assign the physical sites to vertices of a directed tree graph, where cutting edge  $i$  yields a bipartition into subsystem  $\mathcal{L}_i$  and its complement  $\mathcal{R}_i$ . (b) A sequence of  $N-1$  SVDs (11) or, equivalently, QR decompositions then splits off one TTNS tensor  $A_i$  in each step. (c) The resulting tensors are isometries with the orthonormality property (7).

We assign bond vector spaces of dimension  $M_i$  to each edge and assign one tensor  $A_i$  to each vertex. If vertex  $i$  has  $y$  children  $j_1, \dots, j_y$ , then  $A_i$  can be considered a linear map

$$A_i : \mathbb{C}^{M_i} \rightarrow \mathbb{C}^{d_i} \otimes \mathbb{C}^{M_{j_1}} \otimes \dots \otimes \mathbb{C}^{M_{j_y}} \quad (5)$$

from the bond- $i$  vector space to the tensor product of the physical site- $i$  vector space and the child bond vector spaces. The tensor elements can be labeled as

$$[A_i^{\sigma_i}]_{(\mu_{j_1}, \dots, \mu_{j_y}), \mu_i} \quad \text{with} \quad \sigma_i = 1, \dots, d_i, \quad \text{and} \quad \mu_j = 1, \dots, M_j. \quad (6)$$

For the root tensor  $A_N$ , we can set  $M_N = 1$  and interpret  $A_N$  as a pure quantum state (vector) on which the linear maps  $A_{N-1}, \dots, A_1$  act to generate the TTNS in the Hilbert space  $\mathcal{H}$ . Equivalently, the TTNS in the basis  $\{|\sigma_1, \dots, \sigma_N\rangle\}$  is the product of the tensor elements (6), summed over all bond indices  $\mu_1, \dots, \mu_{N-1}$ . For a TTNS with “internal” tensors  $A_i$  that do not carry a physical index, we can set the corresponding site-space dimensions to  $d_i = 1$ .

We say that the TTNS is in canonical form with vertex  $N$  as the orthogonality center [10], if all tensors  $A_i$  are partial isometries and their adjoints  $A_i^\dagger$  are (injective) isometries, i.e., if we have the orthonormality conditions

$$A_i^\dagger A_i \equiv \sum_{\sigma} A_i^{\sigma\dagger} A_i^{\sigma} = 1_{M_i}. \quad (7)$$

### 3. Exact TTNS representation

We want to obtain an exact TTNS representation of a normalized quantum state

$$|\psi\rangle = \sum_{\sigma_1, \dots, \sigma_N} \Psi^{\sigma_1, \dots, \sigma_N} |\sigma_1, \dots, \sigma_N\rangle. \quad (8)$$

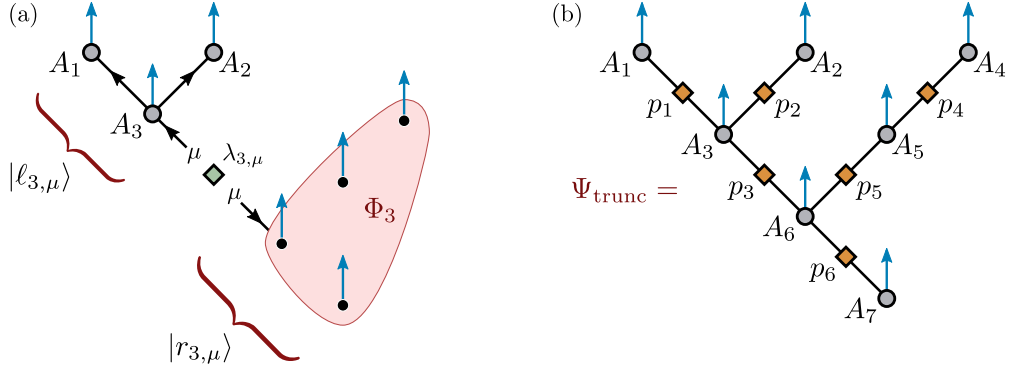


FIG. 2. (a) The SVD (11) for edge  $i$  yields a Schmidt decomposition (9) of the target state  $|\psi\rangle$  with the TTNS formed by tensors  $\{A_j \mid j \in \mathcal{L}(i)\}$  providing an orthonormal basis  $\{|\ell_{i,\mu}\rangle\}$  for subsystem  $\mathcal{L}(i)$  – in this case, sites 1, 2 and 3. Similarly, tensor  $\Phi_i$  provides an orthonormal basis  $\{|r_{i,\mu}\rangle\}$  for subsystem  $\mathcal{R}(i)$  – in this case, sites 4, 5, 6 and 7. (b) The truncated TTNS (23) is obtained from the exact TTNS representation of the target state by inserting projection operators  $p_i$  at every edge, only retaining the  $M_i$ -dimensional bond subspace corresponding to the largest Schmidt coefficients  $\lambda_{i,1} \geq \dots \geq \lambda_{i,M_i}$ .

This can be achieved by a sequence of  $i = 1, \dots, N - 1$  SVDs, each corresponding to a Schmidt decomposition

$$|\psi\rangle = \sum_{\mu} \lambda_{i,\mu} |\ell_{i,\mu}\rangle \otimes |r_{i,\mu}\rangle \quad \text{with Schmidt coefficients} \quad 1 \geq \lambda_{i,1} \geq \lambda_{i,2} \geq \dots \geq 0 \quad (9)$$

and orthonormal bases

$$\{|\ell_{i,\mu}\rangle\}_{\mu} \quad \text{and} \quad \{|r_{i,\mu}\rangle\}_{\mu} \quad (10)$$

for the subsystems  $\mathcal{L}(i)$  and  $\mathcal{R}(i)$ , respectively, corresponding to a cut of edge  $i$  as defined in Section 2.

On the level of the expansion coefficients  $\Psi =: \Psi_0$  and TTNS tensors, this means

$$\Psi_{i-1}^{\sigma_1, \dots, \sigma_N} \stackrel{\text{SVD}}{=} A_i^{\sigma_i} \lambda_i \Phi_i^{\sigma_{i+1}, \dots, \sigma_N} \quad \text{and we define} \quad \Psi_{i-1}^{\sigma_{i+1}, \dots, \sigma_N} := \lambda_i \Phi_i^{\sigma_{i+1}, \dots, \sigma_N} \quad (11)$$

for the next SVD as visualized in Figs. 1b and 2. Here, we only wrote physical indices but no bond indices,  $A_i$  obeys the orthonormality condition (7),  $\lambda_i$  is the diagonal matrix of Schmidt coefficients on the bond vector space of edge  $i$ . The tensor network formed by the tensors  $\{A_j \mid j \in \mathcal{L}(i)\}$  with fixed index  $\mu$  on bond  $i$  gives the state  $|\ell_{i,\mu}\rangle$  from Eq. (9) and  $\Phi_i$  is the tensor of expansion coefficients for the states  $|r_{i,\mu}\rangle$ . See Fig. 2a. Orthonormality  $\langle \ell_{i,\mu} | \ell_{i,\mu'} \rangle = \delta_{\mu,\mu'}$  and  $\langle r_{i,\mu} | r_{i,\mu'} \rangle = \delta_{\mu,\mu'}$  of these states follows from Eq. (7) and an analog orthonormality property of the tensor  $\Phi_i$ , respectively.

#### 4. Lower bounds on error and bond dimensions of truncated TTNS

The lower bound on the approximation accuracy  $\delta := \|\psi - \psi_{\text{TTNS}}\|^2$  in Eq. (1) follows from the Eckart–Young–Mirsky theorem [64]: The best rank- $M_i$  approximation to the target state  $|\psi\rangle$  is given by retaining the  $M_i$  largest Schmidt components of the decomposition (9). Hence,  $\delta$  is bounded from below by each of the rank- $M_i$  truncation errors (2).

Similarly, in order to obtain a TTNS approximation with accuracy  $\delta$ , the bond dimension for edge  $i$  cannot be so small that the single-edge truncation error already exceeds  $\delta$ , i.e.,  $M_i \geq \min\{M \mid \varepsilon_i(M) \leq \delta\}$ . This is the lower bound in Eq. (3).

## 5. Lazy upper bound on error of truncated TTNS

In general, bond dimensions for the exact TTNS representation of Section 3 grow exponentially in the system size  $N$ . We are interested in efficient TTNS approximations and want to determine the upper bounds on the error introduced by truncating bond dimensions to some given values  $M_1, \dots, M_{N-1}$  or, conversely, want to determine useful upper bounds on bond dimensions  $M_i$  that allow for TTNS approximations of a certain accuracy.

One approach is to simply truncate the bond vector space of edge  $i$  in each of the Schmidt decompositions (9) to dimension  $M_i$ , i.e., only retain the  $M_i$  largest singular values before proceeding to the decomposition for edge  $i+1$ . In this way, we generate a sequence of truncated states

$$|\psi\rangle \equiv |\psi_0\rangle \mapsto |\psi_1\rangle \mapsto |\psi_2\rangle \mapsto \dots \mapsto |\psi_{N-1}\rangle, \quad (12)$$

where  $|\psi_{N-1}\rangle$  is a TTNS with bond dimensions  $\{M_i\}$ . Each truncation introduces an error

$$\varepsilon'_i(M_i) := \|\psi_i - \psi_{i-1}\|^2 = \sum_{\mu > M_i} (\lambda'_{i,\mu})^2. \quad (13)$$

Here, primes indicate that the Schmidt coefficients  $\lambda'_{i,\mu}$  of state  $|\psi_{i-1}\rangle$  generally deviate from the exact Schmidt coefficients  $\lambda_{i,\mu}$  of the target state  $|\psi\rangle$  in Eq. (9).

The approximation accuracy can be determined using the telescoping sum

$$|\psi\rangle - |\psi_{N-1}\rangle = \underbrace{|\psi_0\rangle - |\psi_1\rangle}_{=:|\Delta'_1\rangle} + \underbrace{|\psi_1\rangle - |\psi_2\rangle}_{=:|\Delta'_2\rangle} + \dots + \underbrace{|\psi_{N-2}\rangle - |\psi_{N-1}\rangle}_{=:|\Delta'_{N-1}\rangle}. \quad (14)$$

Now,  $|\Delta'_i\rangle$  is orthogonal to  $|\Delta'_j\rangle$  for all  $j > i$  because  $|\psi_i\rangle$  and all its successors have no support on the corresponding discarded subspace for subsystem  $\mathcal{L}(i)$ . Hence, repeated application of the Pythagorean theorem yields the approximation accuracy

$$\|\psi - \psi_{N-1}\|^2 = \|\Delta'_1\|^2 + \dots + \|\Delta'_{N-1}\|^2 = \sum_{i=1}^{N-1} \varepsilon'_i(M_i). \quad (15)$$

## 6. Proper upper bound on error of truncated TTNS

While Eq. (15) nicely connects the approximation accuracy to Schmidt spectra of the states  $|\psi_i\rangle$  in Eq. (12) and is similar to the upper bound in Eq. (1), there is one important caveat: We want to bound TTNS approximation errors and necessary bond dimensions using the Schmidt spectra and Rényi entanglement entropies of the target state  $|\psi\rangle$  itself. Of course, the Schmidt spectra and entanglement entropies of the truncated states  $|\psi_i\rangle$  should be similar to those of the target state  $|\psi\rangle$  if truncation errors are chosen small enough. However, tight continuity bounds for Rényi entropies due to Audenaert involve the Hilbert space dimension [65] (see also Refs. [66–68]), reducing their value and the practicability of Eq. (15) for our purposes.

**MPS.**— In Ref. [32], Verstraete and Cirac established an approximation accuracy bound for MPS based on the Schmidt spectra  $\lambda_i$  of the target state  $|\psi\rangle$ : An exact MPS representation  $\Psi^{\sigma_1, \dots, \sigma_N} = A_1^{\sigma_1} A_2^{\sigma_2} \dots A_N^{\sigma_N}$  can be constructed as described in Section 3 for the special case of a linear graph (every vertex  $i > 1$  having exactly one child  $i-1$  such that  $\mathcal{L}(i) = [1, i]$  and  $\mathcal{R}(i) = [i+1, N]$ ). Inserting at every bond  $i$  a projection

$$[p_i]_{\mu, \mu'} = \begin{cases} \delta_{\mu, \mu'} & \text{if } \mu \leq M_i, \\ 0 & \text{otherwise} \end{cases} \quad (16)$$

onto the subspace corresponding to the  $M_i$  largest Schmidt coefficients  $\lambda_{i,\mu}$ , we obtain the truncated matrix product  $\Psi_{\text{trunc}}^{\sigma_1, \dots, \sigma_N} = \tilde{A}_1^{\sigma_1} \tilde{A}_2^{\sigma_2} \dots \tilde{A}_N^{\sigma_N}$ , where  $\tilde{A}_i^\sigma := p_{i-1} A_i^\sigma p_i$  is the upper-left  $M_{i-1} \times M_i$  block of the matrix  $A_i^\sigma$ . Verstraete and Cirac wrote the overlap of the target state  $|\psi\rangle$  and the truncated MPS  $|\psi_{\text{trunc}}\rangle$  with a sequence of quantum channels

$$\langle \psi | \psi_{\text{trunc}} \rangle = \Psi^\dagger \Psi_{\text{trunc}} = \mathcal{E}_1(\mathcal{E}_2(\dots \mathcal{E}_{N-2}(\mathcal{E}_{N-1}(\lambda_{N-1}^2 p_{N-1}) p_{N-2}) \dots p_2) p_1), \quad (17)$$

where the quantum channels

$$\mathcal{E}_i(\rho) := \sum_{\sigma} A_i^\sigma \rho A_i^{\sigma\dagger} \quad \text{have the property} \quad \mathcal{E}_i(\lambda_i^2) = \lambda_{i-1}^2 \quad (18)$$

due to Eq. (11). Using this property, a short calculation yields the MPS approximation accuracy

$$\|\psi - \psi_{\text{trunc}}\|^2 \leq 2 \sum_i \sum_{\mu > M_i} \lambda_{i,\mu}^2. \quad (19)$$

See also the appendix of Ref. [69].

**TTNS.**— This approach does not work for TTNS that comprise vertices  $i$  with multiple children because a corresponding quantum channel  $\mathcal{E}_i$ , mapping into the tensor product of the children's bond vector spaces, does not have the property from Eq. (18). Instead, we can proceed as follows.

Starting from the exact TTNS representation of the target state  $|\psi\rangle$  constructed in Section 3 and the Schmidt decompositions (9), we can define one projection operator

$$\hat{P}_i := \sum_{\mu \leq M_i} |\ell_{i,\mu}\rangle \langle \ell_{i,\mu}| \otimes \mathbb{1}_{\mathcal{R}(i)} \quad (20)$$

for every edge  $i = 1, \dots, N-1$  of the tree graph.  $\hat{P}_i$  acts non-trivially on subsystem  $\mathcal{L}(i)$  (the branch of vertex  $i$ ) and as the identity on subsystem  $\mathcal{R}(i)$  (the remainder). Specifically,

$$\hat{P}_i |\psi\rangle \stackrel{(9)}{=} \sum_{\mu \leq M_i} \lambda_{i,\mu} |\ell_{i,\mu}\rangle \otimes |r_{i,\mu}\rangle \quad (21)$$

is the original exact TTNS with the sum over bond index  $\mu_i$  restricted to the range  $[1, M_i]$ , corresponding to the  $M_i$  largest Schmidt coefficients  $\lambda_{i,1}, \dots, \lambda_{i,M_i}$ . Equivalently,  $\hat{P}_i |\psi\rangle$  is obtained by inserting the projector  $p_i$  from Eq. (16) on edge  $i$  of the exact TTNS representation. The associated truncation error is

$$\|(1 - \hat{P}_i) |\psi\rangle\|^2 = \sum_{\mu > M_i} \lambda_{i,\mu}^2 \stackrel{(2)}{=} \varepsilon_i(M_i). \quad (22)$$

The truncated TTNS, as illustrated in Fig. 2b, is obtained from the exact representation by restricting all bond indices  $\mu_1, \mu_2, \dots, \mu_{N-1}$  *simultaneously* to the ranges  $\mu_i = 1, \dots, M_i$ . It can be written in the form

$$|\psi_{\text{trunc}}\rangle = \hat{P}_1 \hat{P}_2 \dots \hat{P}_{N-1} |\psi\rangle. \quad (23)$$

The projectors  $\{\hat{P}_i\}$  generally do not commute, and the sequence is essential for the equivalence of Eq. (23) to the simultaneous insertion of bond-space projectors  $p_i$  in the TTNS. In this sequence, projector  $\hat{P}_i$  does not influence the tensors of vertices  $j < i$ ; hence, a subsequent action of a projector  $\hat{P}_{j < i}$  still corresponds exactly to the insertion of  $p_j$  on edge  $j$  of the TTNS.

Using a telescoping sum, the difference from the target state can be written as

$$\begin{aligned}
|\psi\rangle - |\psi_{\text{trunc}}\rangle &= (1 - \hat{P}_1 \hat{P}_2 \cdots \hat{P}_{N-1})|\psi\rangle \\
&= (1 - \hat{P}_1)|\psi\rangle + \hat{P}_1(1 - \hat{P}_2 \hat{P}_3 \cdots \hat{P}_{N-1})|\psi\rangle = \dots \\
&= \underbrace{(1 - \hat{P}_1)|\psi\rangle}_{=:\Delta_1} + \underbrace{\hat{P}_1(1 - \hat{P}_2)|\psi\rangle}_{=:\Delta_2} + \dots + \underbrace{\hat{P}_1 \hat{P}_2 \cdots \hat{P}_{N-2}(1 - \hat{P}_{N-1})|\psi\rangle}_{=:\Delta_{N-1}}. \quad (24)
\end{aligned}$$

The deviation  $|\Delta_1\rangle$  is orthogonal to all  $|\Delta_{j>1}\rangle$ . Due to the non-commuting projectors,  $|\Delta_{i>1}\rangle$  is generally *not* orthogonal to all  $|\Delta_j\rangle$  with  $j > i$ . However, we can still bound the approximation accuracy through repeated application of the Pythagorean theorem  $\|(1 - \hat{P})|\psi\rangle + \hat{P}|\phi\rangle\|^2 = \|(1 - \hat{P})|\psi\rangle\|^2 + \|\hat{P}|\phi\rangle\|^2$  and the contractive property  $\|\hat{P}|\phi\rangle\| \leq \|\phi\|$  of orthogonal projections. With the definition

$$|\phi_i\rangle := (1 - \hat{P}_i)|\psi\rangle + \hat{P}_i(1 - \hat{P}_{i+1})|\psi\rangle + \dots + \hat{P}_i \hat{P}_{i+1} \cdots \hat{P}_{N-2}(1 - \hat{P}_{N-1})|\psi\rangle, \quad (25)$$

we have

$$\begin{aligned}
\|\psi - \psi_{\text{trunc}}\|^2 &\stackrel{(24)}{=} \|\phi_1\|^2 = \|(1 - \hat{P}_1)|\psi\rangle\|^2 + \|\hat{P}_1|\phi_2\rangle\|^2 \\
&\leq \|(1 - \hat{P}_1)|\psi\rangle\|^2 + \|\phi_2\|^2 \\
&= \|(1 - \hat{P}_1)|\psi\rangle\|^2 + \|(1 - \hat{P}_2)|\psi\rangle\|^2 + \|\hat{P}_2|\phi_3\rangle\|^2 \\
&\leq \dots \leq \sum_{i=1}^{N-1} \|(1 - \hat{P}_i)|\psi\rangle\|^2 \stackrel{(22)}{=} \sum_{i=1}^{N-1} \varepsilon_i(M_i). \quad (26)
\end{aligned}$$

From the main result stated in Section 1, this proves upper bounds on the achievable approximation accuracy and required bond dimensions in Eqs. (1) and (3) expressed in terms of truncation errors (2). For the bond-dimension bound in Eq. (3), we have chosen to distribute errors evenly across bonds ( $\varepsilon_i \leq \epsilon$  for all bonds  $i$ ). For MPS, note that the error bound (26) is 1/2 of the original bound (19) by Verstraete and Cirac [32].

## 7. Bounds in terms of Rényi entanglement entropies

A central idea in Refs. [32, 33] on MPS was to relate the truncation error (2) for bond  $i$  to the associated single-branch-cut Rényi entanglement entropy

$$S_\alpha(\rho_i) = \frac{1}{1 - \alpha} \ln \sum_\mu \rho_{i,\mu}^\alpha \quad (\alpha > 0) \quad (27)$$

of the target state  $|\psi\rangle$  for a bipartition into subsystems  $\mathcal{L}(i)$  and  $\mathcal{R}(i)$ . Here,

$$\rho_{i,\mu} := \lambda_{i,\mu}^2 \quad \text{with} \quad \rho_{i,1} \geq \rho_{i,2} \geq \dots \geq 0 \quad \text{and} \quad \sum_\mu \rho_{i,\mu} = 1 \quad (28)$$

denote the decreasingly ordered eigenvalues of the corresponding reduced density matrices, and the truncation error (2) for bond dimension  $M_i$  takes the form  $\varepsilon(\rho_i, M_i) = \sum_{\mu > M_i} \rho_{i,\mu}$ . The Rényi entropy  $S_\alpha$  is Schur-concave [70] such that  $S_\alpha(\rho) \leq S_\alpha(\rho')$  if the distribution  $\rho$  majorizes  $\rho'$ , i.e., if  $\sum_{\mu=1}^m \rho_\mu \geq \sum_{\mu=1}^m \rho'_\mu \forall_m$ .

**Lower bounds on error and bond dimensions.** — For a given TTNS bond dimension  $M_i$  and truncation error  $\delta := \varepsilon(\rho_i, M_i)$ , we can bound  $S_\alpha(\rho_i)$  from *above* by considering the set of

all distributions  $\rho$  that have the truncation error  $\varepsilon(\rho, M_i) = \delta$  and finding the element  $\rho'$  that is majorized by all others. The distribution  $\rho'$  has to be as spread out as possible, i.e., takes the form [33]

$$\rho'_\mu = \begin{cases} (1 - \epsilon)/M_i & \text{for } \mu = 1, \dots, M_i \text{ and} \\ \delta/(D - M_i) & \text{for } \mu = M_i + 1, \dots, D, \end{cases} \quad (29)$$

where  $D$  is the available Hilbert space dimension (the smaller of the dimensions of the Hilbert spaces for subsystems  $\mathcal{L}_i$  and  $\mathcal{R}_i$ ). Hence,

$$\begin{aligned} S_\alpha(\rho_i) \leq S_\alpha(\rho') &= \frac{1}{1 - \alpha} \ln \left[ M_i \left( \frac{1 - \delta}{M_i} \right)^\alpha + (D - M_i) \left( \frac{\delta}{D - M_i} \right)^\alpha \right] \\ &\leq \ln M_i + \frac{\alpha}{1 - \alpha} \ln(1 - \delta) \quad \text{if } \alpha > 1. \end{aligned} \quad (30)$$

The constraint  $\alpha > 1$  on the Rényi parameter is needed for the second inequality. Inequality (30) establishes the lower bounds on the achievable approximation accuracy and required bond dimensions in terms of Rényi entanglement entropies  $S_\alpha$  as stated in Eqs. (1) and (3) of the main result.

**Upper bounds on error and bond dimensions.** — Similarly, for a given TTNS bond dimension  $M_i$ , truncation error  $\epsilon := \varepsilon(\rho_i, M_i)$ , and probability  $p := \rho_{i,M_i}$ , we can bound  $S_\alpha(\rho_i)$  from below by considering the set of all distributions  $\rho$  that have the truncation error  $\varepsilon(\rho, M_i) = \epsilon$  and  $\rho_{M_i} = p$ , and finding the element  $\tilde{\rho}$  that majorizes all others. As discussed in Refs. [32, 69], this leads to the bound

$$S_\alpha(\rho_i) \geq S_\alpha(\tilde{\rho}) \geq \frac{1}{1 - \alpha} \ln [(M_i - 1)^{1 - \alpha} \epsilon^\alpha], \quad (31)$$

where the second inequality holds if

$$1 > \alpha \geq \frac{\epsilon M_i}{M_i - 1 - \epsilon}. \quad (32)$$

For the practically interesting case of small  $\epsilon$  and large  $M_i$ , the lower boundary of this  $\alpha$  interval is approximately  $\epsilon$ .

The inequality (31) can be used to bound the TTNS truncation error  $\epsilon$  from above for a given bond dimension  $M_i$  or to bound  $M_i$  from above for a given desired truncation error  $\epsilon$ . From the main result stated in Section 1, this yields the upper bounds on the achievable approximation accuracy and required bond dimensions expressed in terms of Rényi entanglement entropies  $S_\alpha$  in Eqs. (1) and (3).

If Rényi entanglement entropies  $S_{\alpha,i}$  are known for several values of the parameter  $\alpha$ , one can optimize the bounds (30) and (31) with respect to  $\alpha$ .

## 8. Conclusion

The main result stated in the introduction provides rigorous bounds (1) on the attainable TTNS approximation accuracy for given bond dimensions and, conversely, bounds (3) on TTNS bond dimensions needed to achieve a certain approximation accuracy. The bounds can be formulated in terms of the target state's Schmidt spectra or (less tightly) in terms of  $\alpha$ -Rényi entanglement entropies  $S_{\alpha,i}$  with  $\alpha < 1$  for upper bounds and  $\alpha > 1$  for lower bounds.

If the target state obeys an *entanglement area law* or *log-area law*, then the presented bounds imply the existence of efficient faithful TTNS approximations. Specifically, for a certain

assignment of physical sites to vertices of a tree graph, the entanglement entropies  $S_{\alpha,i}$  for cutting the tree at any edge  $i$  should have an upper bound

$$S_{\alpha,i} < C \quad (\text{area law}) \quad \text{or} \quad S_{\alpha,i} < c \ln N \quad (\text{log-area law}) \quad \forall 1 \leq i < N \quad (33)$$

with some size-independent real constants  $C$  and  $c > 0$ , respectively. Then, TTNS approximations exist for any required accuracy, with bond dimensions growing at most polynomially in the system size  $N$ .

If the target-state entanglement across some edges grows polynomially in the system size, the lower bound in Eq. (3) implies that the associated TTNS bond dimensions need to increase exponentially in  $N$ .

For *low-energy states of gapped systems* with finite-range interactions on a tree graph, one generally expects an entanglement area law if correlation lengths are sufficiently short compared to the average vertex degree. The situation is somewhat more nuanced in comparison to one-dimensional systems, where the entanglement area law holds independent of the (finite) amplitude of correlation lengths [71, 72]. For multiple gapped spin systems on trees with vertex degree  $z$ , numerical studies in Refs. [73–75] report groundstate correlation lengths  $\xi$  bounded from above by  $\xi_0 = 1/\ln(z-1)$ , which suggests an entanglement area law. Note that the products  $(z-1)^\ell e^{-\ell\xi}$  of the volume growth factor and correlation decay, which appear in entanglement bounds à la Hastings [71], may diverge for correlation lengths  $\xi > \chi_0$  with increasing distance  $\ell$  from the cut tree edge. In Ref. [76] volume-law entanglement  $S_{\alpha,i} \sim c'N$  was observed in the ground states of gapless fermionic systems on Bethe lattices.

If the target state does not obey an entanglement (log-)area law, the derived bounds can still be useful to *estimate TTNS computation costs* and control bond dimensions, or to *optimize the tree graph structure* [28, 41, 50, 52, 77, 78] to reduce the computation costs.

While the bounds on approximation accuracy and required bond dimensions can guarantee the existence of efficient TTNS approximations, we do not necessarily have *efficient methods* for finding these approximations. For the variational optimization of groundstate approximations, DMRG algorithms [17, 19, 27, 28, 39] generally work well and we do not expect that more practical methods exist for unconstrained TTNS, but there is no fundamental theory for the convergence of DMRG. Concerning MPS groundstate search for one-dimensional gapped local Hamiltonians, Landau, Vazirani, and Vidick devised a provably polynomial-time algorithm [79]. It is conceivable that this can be extended to TTNS groundstate search for local Hamiltonians on trees with a sufficiently large energy gap.

Finally, the presented bounds apply to the case of unconstrained tensors and would generally need adaptation for *TTNS with tensor constraints* such as restrictions on CP ranks [80, 81].

### Acknowledgments

I thank Elizabeth Bennewitz, Zohreh Davoudi, Alexey Gorshkov, So-Yun Jang, Hersh Kumar, Alessio Lerose, Benjamin Lovitz, Federica Surace, and Nikita Zemlevskiy for discussions that motivated this work.

---

[1] H. A. Kramers and G. H. Wannier, *Statistics of the two-dimensional ferromagnet. Part II*, *Phys. Rev.* **60**, 263 (1941).

[2] R. J. Baxter, *Dimers on a rectangular lattice*, *J. Math. Phys.* **9**, 650 (1968).

[3] M. P. Nightingale and H. W. J. Blöte, *Gap of the linear spin-1 Heisenberg antiferromagnet: A Monte Carlo calculation*, *Phys. Rev. B* **33**, 659 (1986).

[4] M. Fannes, B. Nachtergael, and R. F. Werner, *Finitely correlated states on quantum spin chains*, *Commun. Math. Phys.* **144**, 443 (1992).

[5] S. R. White, *Density matrix formulation for quantum renormalization groups*, *Phys. Rev. Lett.* **69**, 2863 (1992).

[6] H. Niggemann, A. Klümper, and J. Zittartz, *Quantum phase transition in spin-3/2 systems on the hexagonal lattice - optimum ground state approach*, *Z. Phys. B* **104**, 103 (1997).

[7] T. Nishino, K. Okunishi, Y. Hieida, N. Maeshima, and Y. Akutsu, *Self-consistent tensor product variational approximation for 3D classical models*, *Nucl. Phys. B* **575**, 504 (2000).

[8] F. Verstraete and J. I. Cirac, *Renormalization algorithms for quantum-many body systems in two and higher dimensions*, [arXiv:cond-mat/0407066](https://arxiv.org/abs/cond-mat/0407066) (2004).

[9] G. Vidal, *Entanglement renormalization*, *Phys. Rev. Lett.* **99**, 220405 (2007).

[10] U. Schollwöck, *The density-matrix renormalization group in the age of matrix product states*, *Ann. Phys.* **326**, 96 (2011).

[11] R. Orús, *A practical introduction to tensor networks: Matrix product states and projected entangled pair states*, *Ann. Phys.* **349**, 117 (2014).

[12] J. I. Cirac, D. Pérez-García, N. Schuch, and F. Verstraete, *Matrix product states and projected entangled pair states: Concepts, symmetries, and theorems*, *Rev. Mod. Phys.* **93**, 045003 (2021).

[13] S. R. White, *Density-matrix algorithms for quantum renormalization groups*, *Phys. Rev. B* **48**, 10345 (1993).

[14] S. Östlund and S. Rommer, *Thermodynamic limit of density-matrix renormalization*, *Phys. Rev. Lett.* **75**, 3537 (1995).

[15] S. Rommer and S. Östlund, *A class of ansatz wave functions for 1D spin systems and their relation to DMRG*, *Phys. Rev. B* **55**, 2164 (1997).

[16] I. Affleck, T. Kennedy, E. H. Lieb, and H. Tasaki, *Rigorous results on valence-bond ground states in antiferromagnets*, *Phys. Rev. Lett.* **59**, 799 (1987).

[17] H. Otsuka, *Density-matrix renormalization-group study of the spin-1/2 XXZ antiferromagnet on the Bethe lattice*, *Phys. Rev. B* **53**, 14004 (1996).

[18] B. Friedman, *A density matrix renormalization group approach to interacting quantum systems on Cayley trees*, *J. Phys. Condens. Matter* **9**, 9021 (1997).

[19] M.-B. Lepetit, M. Cousy, and G. M. Pastor, *Density-matrix renormalization study of the Hubbard model on a Bethe lattice*, *Eur. Phys. J. B* **13**, 421 (2000).

[20] L. P. Kadanoff, *Scaling laws for Ising models near  $T_c$* , *Physics* **2**, 263 (1966).

[21] R. Jullien, J. Fields, and S. Doniach, *Kondo lattice: Real-space renormalization-group approach*, *Phys. Rev. Lett.* **38**, 1500 (1977).

[22] S. D. Drell, M. Weinstein, and S. Yankielowicz, *Quantum field theories on a lattice: Variational methods for arbitrary coupling strengths and the Ising model in a transverse magnetic field*, *Phys. Rev. D* **16**, 1769 (1977).

[23] M. E. Fisher, *Renormalization group theory: Its basis and formulation in statistical physics*, *Rev. Mod. Phys.* **70**, 653 (1998).

[24] M. Fannes, B. Nachtergael, and R. F. Werner, *Ground states of VBS models on Cayley trees*, *J. Stat. Phys.* **66**, 939 (1992).

[25] Y.-Y. Shi, L.-M. Duan, and G. Vidal, *Classical simulation of quantum many-body systems with a tree tensor network*, *Phys. Rev. A* **74**, 022320 (2006).

[26] L. Tagliacozzo, G. Evenbly, and G. Vidal, *Simulation of two-dimensional quantum systems using a tree tensor network that exploits the entropic area law*, *Phys. Rev. B* **80**, 235127 (2009).

[27] V. Murg, F. Verstraete, O. Legeza, and R. M. Noack, *Simulating strongly correlated quantum systems with tree tensor networks*, *Phys. Rev. B* **82**, 205105 (2010).

[28] N. Nakatani and G. K.-L. Chan, *Efficient tree tensor network states (TTNS) for quantum chemistry*:

*Generalizations of the density matrix renormalization group algorithm*, *J. Chem. Phys.* **138**, 134113 (2013).

[29] T. Barthel, J. Lu, and G. Friesecke, *On the closedness and geometry of tensor network state sets*, *Lett. Math. Phys.* **112**, 72 (2022).

[30] T. Barthel and Q. Miao, *Absence of barren plateaus and scaling of gradients in the energy optimization of isometric tensor network states*, *Commun. Math. Phys.* **406**, 86 (2025).

[31] Q. Miao and T. Barthel, *Isometric tensor network optimization for extensive Hamiltonians is free of barren plateaus*, *Phys. Rev. A* **109**, L050402 (2024).

[32] F. Verstraete and J. I. Cirac, *Matrix product states represent ground states faithfully*, *Phys. Rev. B* **73**, 094423 (2006).

[33] N. Schuch, M. M. Wolf, F. Verstraete, and J. I. Cirac, *Entropy scaling and simulability by matrix product states*, *Phys. Rev. Lett.* **100**, 030504 (2008).

[34] D. Bauernfeind, M. Zingl, R. Triebel, M. Aichhorn, and H. G. Evertz, *Fork tensor-product states: efficient multiorbital real-time DMFT solver*, *Phys. Rev. X* **7**, 031013 (2017).

[35] M. Gerster, M. Rizzi, P. Silvi, M. Dalmonte, and S. Montangero, *Fractional quantum Hall effect in the interacting Hofstadter model via tensor networks*, *Phys. Rev. B* **96**, 195123 (2017).

[36] E. Macaluso, T. Comparin, R. O. Umucalilar, M. Gerster, S. Montangero, M. Rizzi, and I. Carusotto, *Charge and statistics of lattice quasiholes from density measurements: A tree tensor network study*, *Phys. Rev. Res.* **2**, 013145 (2020).

[37] D. Bauernfeind and M. Aichhorn, *Time dependent variational principle for tree tensor networks*, *SciPost Phys.* **8**, 024 (2020).

[38] B. Kloss, D. Reichman, and Y. Bar Lev, *Studying dynamics in two-dimensional quantum lattices using tree tensor network states*, *SciPost Phys.* **9**, 070 (2020).

[39] X. Cao, Y. Lu, P. Hansmann, and M. W. Haverkort, *Tree tensor-network real-time multiorbital impurity solver: Spin-orbit coupling and correlation functions in  $Sr_2RuO_4$* , *Phys. Rev. B* **104**, 115119 (2021).

[40] T. Felser, S. Notarnicola, and S. Montangero, *Efficient tensor network ansatz for high-dimensional quantum many-body problems*, *Phys. Rev. Lett.* **126**, 170603 (2021).

[41] T. Hikihara, H. Ueda, K. Okunishi, K. Harada, and T. Nishino, *Automatic structural optimization of tree tensor networks*, *Phys. Rev. Res.* **5**, 013031 (2023).

[42] M. Grundner, P. Westhoff, F. B. Kugler, O. Parcollet, and U. Schollwöck, *Complex time evolution in tensor networks and time-dependent Green's functions*, *Phys. Rev. B* **109**, 155124 (2024).

[43] D. Sulz, C. Lubich, G. Ceruti, I. Lesanovsky, and F. Carollo, *Numerical simulation of long-range open quantum many-body dynamics with tree tensor networks*, *Phys. Rev. A* **109**, 022420 (2024).

[44] L. Pavešić, D. Jaschke, and S. Montangero, *Constrained dynamics and confinement in the two-dimensional quantum Ising model*, *Phys. Rev. B* **111**, L140305 (2025).

[45] W. Krinitzin, N. Tausendpfund, M. Heyl, M. Rizzi, and M. Schmitt, *Time evolution of the quantum Ising model in two dimensions using tree tensor networks*, *Phys. Rev. B* **112**, 134310 (2025).

[46] W. Krinitzin, N. Tausendpfund, M. Rizzi, M. Heyl, and M. Schmitt, *Roughening dynamics of interfaces in the two-dimensional quantum Ising model*, *Phys. Rev. Lett.* **134**, 240402 (2025).

[47] L. Pavešić, M. Di Liberto, and S. Montangero, *Scattering and induced false vacuum decay in the two-dimensional quantum Ising model*, *arXiv:2509.02702* (2025).

[48] T. Felser, P. Silvi, M. Collura, and S. Montangero, *Two-dimensional quantum-link lattice quantum electrodynamics at finite density*, *Phys. Rev. X* **10**, 041040 (2020).

[49] G. Magnifico, T. Felser, P. Silvi, and S. Montangero, *Lattice quantum electrodynamics in (3+1)-dimensions at finite density with tensor networks*, *Nat. Commun.* **12**, 3600 (2021).

[50] V. Murg, F. Verstraete, R. Schneider, P. R. Nagy, and O. Legeza, *Tree tensor network state with variable tensor order: An efficient multireference method for strongly correlated systems*, *J. Chem. Theory Comput.* **11**, 1027–1036 (2015).

[51] K. Gunst, F. Verstraete, S. Wouters, O. Legeza, and D. Van Neck, *T3NS: Three-legged tree tensor network states*, *J. Chem. Theory Comput.* **14**, 2026–2033 (2018).

[52] H. R. Larsson, *Computing vibrational eigenstates with tree tensor network states (TTNS)*, *J. Chem. Phys.* **151**, 204102 (2019).

[53] E. Dumitrescu, *Tree tensor network approach to simulating Shor's algorithm*, *Phys. Rev. A* **96**, 062322 (2017).

[54] P. Seitz, I. Medina, E. Cruz, Q. Huang, and C. B. Mendl, *Simulating quantum circuits using tree tensor*

*networks*, *Quantum* **7**, 964 (2023).

[55] D. Jaschke, A. Pagano, S. Weber, and S. Montangero, *Ab-initio tree-tensor-network digital twin for quantum computer benchmarking in 2D*, *Quantum Sci. Technol.* **9**, 035055 (2024).

[56] A. Dubey, Z. Zeybek, and P. Schmelcher, *Simulating quantum circuits with tree tensor networks using density-matrix renormalization group algorithm*, *Phys. Rev. B* **112**, 104312 (2025).

[57] A. Rényi, *On measures of entropy and information*, *Berkeley Symp. on Math. Statist. and Prob.* 547 (1961).

[58] N. Laflorencie, *Quantum entanglement in condensed matter systems*, *Phys. Rep.* **646**, 1 (2016).

[59] T. Barthel, C. Pineda, and J. Eisert, *Contraction of fermionic operator circuits and the simulation of strongly correlated fermions*, *Phys. Rev. A* **80**, 042333 (2009).

[60] P. Corboz and G. Vidal, *Fermionic multiscale entanglement renormalization ansatz*, *Phys. Rev. B* **80**, 165129 (2009).

[61] P. Corboz, G. Evenbly, F. Verstraete, and G. Vidal, *Simulation of interacting fermions with entanglement renormalization*, *Phys. Rev. A* **81**, 010303(R) (2010).

[62] C. Pineda, T. Barthel, and J. Eisert, *Unitary circuits for strongly correlated fermions*, *Phys. Rev. A* **81**, 050303(R) (2010).

[63] C. V. Kraus, N. Schuch, F. Verstraete, and J. I. Cirac, *Fermionic projected entangled pair states*, *Phys. Rev. A* **81**, 052338 (2010).

[64] C. Eckart and G. Young, *The approximation of one matrix by another of lower rank*, *Psychometrika* **1**, 211 (1936).

[65] K. M. R. Audenaert, *A sharp continuity estimate for the von Neumann entropy*, *J. Phys. A: Math. Theor.* **40**, 8127 (2007).

[66] E. P. Hanson and N. Datta, *Tight uniform continuity bound for a family of entropies*, *arXiv:1707.04249* (2017).

[67] A. E. Rastegin, *Some general properties of unified entropies*, *J. Stat. Phys.* **143**, 1120 (2011).

[68] Z. Chen, Z. Ma, I. Nikoufar, and S.-M. Fei, *Sharp continuity bounds for entropy and conditional entropy*, *Sci. China Phys. Mech. Astron.* **60**, 020321 (2017).

[69] T. Barthel, *Typical one-dimensional quantum systems at finite temperatures can be simulated efficiently on classical computers*, *arXiv:1708.09349* (2017).

[70] R. Bhatia, *Matrix Analysis* (Springer, New York, 1997).

[71] M. B. Hastings, *An area law for one-dimensional quantum systems*, *J. Stat. Mech.* P08024 (2007).

[72] F. G. S. L. Brandão and M. Horodecki, *An area law for entanglement from exponential decay of correlations*, *Nat. Phys.* **9**, 721 (2013).

[73] D. Nagaj, E. Farhi, J. Goldstone, P. Shor, and I. Sylvester, *Quantum transverse-field Ising model on an infinite tree from matrix product states*, *Phys. Rev. B* **77**, 214431 (2008).

[74] M. Kumar, S. Ramasesha, and Z. G. Soos, *Density matrix renormalization group algorithm for Bethe lattices of spin- $\frac{1}{2}$  or spin-1 sites with Heisenberg antiferromagnetic exchange*, *Phys. Rev. B* **85**, 134415 (2012).

[75] W. Li, J. von Delft, and T. Xiang, *Efficient simulation of infinite tree tensor network states on the Bethe lattice*, *Phys. Rev. B* **86**, 195137 (2012).

[76] B. Caravan, B. A. Friedman, and G. C. Levine, *Scaling of entanglement entropy in point-contact, free-fermion systems*, *Phys. Rev. A* **89**, 052305 (2014).

[77] G. Cataldi, A. Abedi, G. Magnifico, S. Notarnicola, N. D. Pozza, V. Giovannetti, and S. Montangero, *Hilbert curve vs Hilbert space: exploiting fractal 2D covering to increase tensor network efficiency*, *Quantum* **5**, 556 (2021).

[78] G. Ferrari, G. Magnifico, and S. Montangero, *Adaptive-weighted tree tensor networks for disordered quantum many-body systems*, *Phys. Rev. B* **105**, 214201 (2022).

[79] Z. Landau, U. Vazirani, and T. Vidick, *A polynomial time algorithm for the ground state of one-dimensional gapped local Hamiltonians*, *Nat. Phys.* **11**, 566 (2015).

[80] H. Chen and T. Barthel, *Tensor network states with low-rank tensors*, *arXiv:2205.15296* (2022).

[81] H. Chen and T. Barthel, *Machine learning with tree tensor networks, CP rank constraints, and tensor dropout*, *IEEE Trans. Pattern Anal. Mach. Intell.* **46**, 7825 (2024).